

# SeamlessNeRF: Stitching Part NeRFs with Gradient Propagation

Bingchen Gong\*  
 Yuehao Wang\*  
 gongbingchen@gmail.com  
 yhwang@link.cuhk.edu.hk  
 The Chinese University of Hong Kong  
 Hong Kong, China

Xiaoguang Han†  
 hanxiaoguang@cuhk.edu.cn  
 The Chinese University of Hong Kong  
 (Shenzhen)  
 Shenzhen, China

Qi Dou†  
 qidou@cuhk.edu.hk  
 The Chinese University of Hong Kong  
 Hong Kong, China



**Figure 1:** We demonstrate the appearance blending results of our proposed approach. In the exhibited case (a), we represent the sculptures in radiance fields and aim to repair the “Venus de Milo” sculpture with the arms of another marble statue. In (b), we display the results obtained by a direct concatenation of the target arms and the source sculpture, which incurs incoherence between the new arms and the original one. In (c), our proposed approach can overcome this problem by fusing the source appearance into the target parts.

## ABSTRACT

Neural Radiance Fields (NeRFs) have emerged as promising digital mediums of 3D objects and scenes, sparking a surge in research to extend the editing capabilities in this domain. The task of seamless editing and merging of multiple NeRFs, resembling the “Poisson blending” in 2D image editing, remains a critical operation that is under-explored by existing work. To fill this gap, we propose SeamlessNeRF, a novel approach for seamless appearance blending of multiple NeRFs. In specific, we aim to optimize the appearance of a target radiance field in order to harmonize its merge with a source field. We propose a well-tailored optimization procedure for blending, which is constrained by 1) pinning the radiance color in

the intersecting boundary area between the source and target fields and 2) maintaining the original gradient of the target. Extensive experiments validate that our approach can effectively propagate the source appearance from the boundary area to the entire target field through the gradients. To the best of our knowledge, SeamlessNeRF is the first work that introduces gradient-guided appearance editing to radiance fields, offering solutions for seamless stitching of 3D objects represented in NeRFs. Our code and more results are available at <https://sites.google.com/view/seamlessnerf>.

## CCS CONCEPTS

- Computing methodologies → Reconstruction; Image-based rendering; Volumetric models.

## KEYWORDS

neural radiance fields, gradient propagation, seamless, composition, 3D editing

### ACM Reference Format:

Bingchen Gong, Yuehao Wang, Xiaoguang Han, and Qi Dou. 2023. SeamlessNeRF: Stitching Part NeRFs with Gradient Propagation. In *SIGGRAPH Asia 2023 Conference Papers (SA Conference Papers '23)*, December 12–15, 2023, Sydney, NSW, Australia. ACM, New York, NY, USA, 10 pages. <https://doi.org/10.1145/3610548.3618238>

\*Both authors contributed equally to this work.

†Corresponding authors: hanxiaoguang@cuhk.edu.cn; qidou@cuhk.edu.hk

Permission to make digital or hard copies of all or part of this work for personal or classroom use is granted without fee provided that copies are not made or distributed for profit or commercial advantage and that copies bear this notice and the full citation on the first page. Copyrights for components of this work owned by others than the author(s) must be honored. Abstracting with credit is permitted. To copy otherwise, or republish, to post on servers or to redistribute to lists, requires prior specific permission and/or a fee. Request permissions from [permissions@acm.org](mailto:permissions@acm.org).

*SA Conference Papers '23, December 12–15, 2023, Sydney, NSW, Australia*

© 2023 Copyright held by the owner/author(s). Publication rights licensed to ACM. ACM ISBN 979-8-4007-0315-7/23/12...\$15.00  
<https://doi.org/10.1145/3610548.3618238>

## 1 INTRODUCTION

Neural Radiance Fields (NeRFs) [Mildenhall et al. 2021] have been established as a potent representation of 3D scenes and are widely considered to be the top contender for future media forms, alongside images and videos. Therefore, incorporating basic editing functionalities into this novel representation is of substantial importance.

Seamless stitching and transplantation of a 3D object to another is a fundamental editing operation, akin to the common seamless blending functionality on 2D images. This is a long-standing problem [Rocchini et al. 1999; Yu et al. 2004] as mixing and re-creating 3D models are important steps in gaming, filming, and artistic creation. For instance, as illustrated in Fig. 1, the arms of a ceramic dancing woman can be precisely extracted and seamlessly integrated into the renowned “Venus de Milo” sculpture for building artistic derivative. By this merging process, the texture attributes from the source (the “Venus de Milo”) are propagated into the newly stitched arms, producing a natural and cohesive appearance. Nevertheless, the seamless editing technique is still missing for 3D objects represented in NeRFs. Since appearance information in radiance fields is encoded in black-box network parameters, propagating texture information between source and target implicit fields poses a particular challenge.

Among the various approaches developed to seamlessly merge two images, gradient-based melding techniques stand out due to their robustness to diverse scenarios and user-friendly interactions [Bhat et al. 2010; Darabi et al. 2012; Pérez et al. 2003]. These methods, anchored on the Poisson equation, basically resolve a system of equations to uphold gradient consistency on the intersecting boundary of images and preserve the original image gradients within the boundary. In this way, a smooth transition is imposed between the merged images. In the domain of implicit fields, the manipulation of objectives involving gradients has been established as a viable pursuit, as affirmed by previous work [Li et al. 2023; Xu et al. 2022]. Consequently, gradient-based melding emerges as an attractive option for facilitating the seamless merging of NeRFs.

In this paper, we present SeamlessNeRF, a novel framework designed to facilitate gradient-based appearance blending of NeRFs. Given source and target objects represented in NeRFs, our key idea is to optimize the appearance of the target field to harmonize its texture style with the source field, thereby achieving a smooth transition between the source and target fields. To do this, we begin with transforming the source and target NeRFs into a unified homogeneous coordinate space, followed by constructing a piecewise radiance field based on their density values. During the optimization for appearance blending, the radiance of the source and target are reconciled in their intersecting boundary area. Concurrently, we impose regularization on the gradient field of the target to preserve its original appearance change. This enables the propagation of radiance color from the source to the target through the gradient field. In order to efficiently compute the radiance gradients in the unified 3D space, we resort to finite difference in implicit fields. Since radiance fields are view-dependent, we propose a sampling strategy to identify each point’s view direction. Furthermore, a side-branch fine-tuning scheme is incorporated into the appearance optimization procedure for faster convergence and preserving texture details. In summary, our main contributions include:

- We propose a novel framework for seamlessly stitching part NeRFs into a unified and harmonized 3D representation, which, to our knowledge, is the first of its kind.
- We introduce a gradient propagation method, which preserves the texture patterns that are inherently implied in the gradient fields, and ensures a smooth radiance transition across the boundaries.
- We conduct comprehensive experiments to validate the effectiveness of our approach across a diverse range of scenarios and different backbones.

## 2 RELATED WORK

### 2.1 NeRF Editing

Previous work [Tang et al. 2022; Zhang et al. 2021a] has explored possible solutions to entity placement and composition of NeRF-represented scenes. NeRFShop [Jambon et al. 2023] allows users to interactively select and deform objects through cage-based transformations, where membrane interpolation technique is proposed to reduce potential editing artifacts. Block-NeRF [Tancik et al. 2022] merges multiple radiance fields into one in order to achieve novel view synthesis of large-scale scenes. To composite adjacent radiance fields under different time of day, color balance, and weather, an appearance matching scheme is proposed to align the appearance of the neighboring blocks. However, Block-NeRF considers merging two blocks of the same scene with large overlaps, which diverges from stitching part NeRFs.

Regarding appearance editing in NeRFs, the challenge arises from their implicit scene representations. Previous study [Liu et al. 2021; Xu et al. 2022; Yang et al. 2021; Zheng et al. 2022; Zhuang et al. 2022] focused on purely implicit editing. The approach proposed by [Yuan et al. 2022] extracts explicit meshes as a manipulable proxy to facilitate editing in implicit representations. NeRV [Srinivasan et al. 2021], NeRFactor [Zhang et al. 2021b], SAMURAI [Boss et al. 2022], NVDiffRec [Munkberg et al. 2022], and Ref-NeRF [Verbin et al. 2022] support editable BRDF materials by decoupling 3D geometry and lighting effects from multi-view captures. Other noteworthy progresses in this area, including EditNeRF [Liu et al. 2021] and CodeNeRF [Yang et al. 2021], encode the shape and appearance of simple objects into an interpolative latent code. CLIP-NeRF [Wang et al. 2022] and DFFs [Kobayashi et al. 2022] explored text-guided scene editing utilizing the joint vision-language embedding inherent in the CLIP model [Radford et al. 2021]. Instruct-NeRF2NeRF [Haque et al. 2023] further enhances text-guided NeRF editing by using diffusion models [Brooks et al. 2023]. PaletteNeRF [Kuang et al. 2023] and RecolorNeRF [Gong et al. 2023] enable palette-based color editing for NeRF-represented scenes. Style transferring schemes proposed by UPST-NeRF [Chen et al. 2022b], INS [Fan et al. 2022], StyleRF [Liu et al. 2023], and ARF [Zhang et al. 2022] stylize NeRF models to resemble reference images. NeRFEeditor [Sun et al. 2022a] goes a step further by encoding novel-view images into the hidden space of StyleGAN, supporting editing guided by reference images, text prompts, and user interactions. While the majority of the methods discussed in this section have demonstrated significant capabilities in composition and appearance editing, they struggle when tasked with the seamless stitching and appearance blending of NeRF-represented assets.

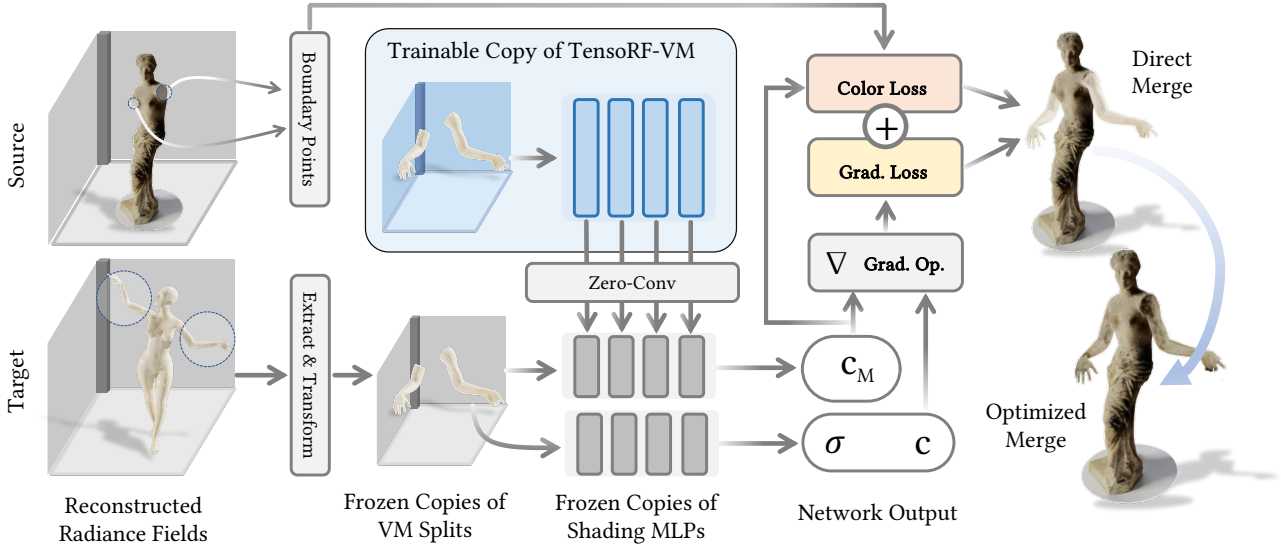


**Figure 2: Pipeline of our proposed approach for seamless appearance blending. We adopt TensoRF-VM [Chen et al. 2022a] as our radiance field backbone. The pipeline enables appearance blending by fine-tuning a trainable copy of the target radiance field, which connects the frozen copies via zero convolutions.**

## 2.2 Seamless Editing

Seamless editing, particularly in the domains of photo and texture editing, has been an area of significant research focus in the field of computer graphics and digital image processing. The aim is to ensure that modifications or blends in the images or textures are smooth and undetectable, thus maintaining their visual coherence. A noteworthy work on this task is the “Poisson Image Editing” by Pérez et al. [2003], where they showcased a gradient-domain color adjustment technique for managing color inconsistencies in image compositing, thereby ensuring seamless transitions. This work was closely followed by Agarwala et al. [2004], which integrates gradient-domain blending with graph cuts, enabling the seamless combination of different sources at interactive speeds for a broad range of compositing applications. Their framework demonstrated success in stitching unrelated photos that possess roughly similar overlapping regions [Kaneva et al. 2010]. Meanwhile, Kwatra et al. [2005] introduces “Texture Optimization” that allows the seamless transfer of photographic textures from an example to a target image, effectively cloning texture patterns. Barnes et al. [2009] put forth “PatchMatch”, an algorithm that enables seamless reshuffling of image regions. The advent of deep learning led to methods like “Deep Image Analogy” by [Liao et al. 2017], which uses convolutional neural networks (CNNs) to find semantically meaningful dense correspondences between two input images, providing more advanced solutions for seamless editing. Regarding seamless editing in 3D objects, Rocchini et al. [1999] and Dessein et al. [2014] propose methods for stitching and blending textures on 3D objects. However, the appearance of NeRFs is encoded in neural networks rather than textures, resulting in challenges to using texture-based approaches. Yu et al. [2004] adopts the Poisson equation to implicitly modify the original mesh geometry through gradient field

manipulation. While this work offers smooth merging in geometry, the appearance blending is not considered. The application of gradient-domain methods is also extended to the spatio-temporal domain by Wang et al. [2007], which primarily focuses on video frames.

In essence, traditional editing techniques degenerate when applied directly to NeRFs as image melding algorithms do not account for occlusion and view consistency in 3D space and existing 3D melding approaches lack essential designs for neural implicit fields.

## 3 SEAMLESS NEURAL RADIANCE FIELDS

Our approach towards creating SeamlessNeRF begins with reconstructing multiple NeRFs from individual sets of multi-view images. We choose TensorF-VM [Chen et al. 2022a] as the NeRF backbone. After the acquisition of 3D assets represented in NeRFs, we aim to merge them into a single harmonized one.

### 3.1 Transforming and Merging Radiance Fields

The first stage involves the transformation and alignment of distinct NeRFs. This stage receives a user-input transformation which will be applied to join the source field  $F_1$  and the target fields  $\{F_i\}_{i=2}^N$ . We assume the coordinate system of the merged object is unified with the source field in a global coordinate system. We apply  $3 \times 4$  affine transformations to align the target fields into the unified global space. This manual alignment plays a role in maintaining the geometric coherence of the merged object, ensuring there are reasonable overlapping areas between the source field and target fields for appearance blending.

Once the transformation is complete, the next stage is to render these aligned fields as a single field  $F_M : (\mathbf{x}, \mathbf{d}) \rightarrow (\mathbf{c}, \sigma)$ . Since each field's coordinate-to-radiance mapping is independent of each

other, a unified mapping for the merged object should be established. Thus, we define the unified field  $F_M$  as a piece-wise function over multiple sub-fields. Intuitively, this piece-wise function should hold the property that sparser space in the source field should be dominated by the densest field in order to allow the target fields to occupy the empty space in the source field. To achieve this, we define a field selector function based on the density:

$$S(\mathbf{x}) = \arg \max_{i=1..N} \beta_i \sigma_i(\mathbf{M}_i \mathbf{x}), \quad (1)$$

where  $N$  is the number of the merging fields,  $\mathbf{M}_i \in \mathbb{R}^{3 \times 4}$  is an affine matrix transforming the  $i$ -th field to the unified global space (note that the transformation of the source field is an identity matrix),  $\beta_i$  is a tunable weight for scaling the precedence order for different fields. Higher  $\beta_i$  indicates higher precedence of the  $i$ -th field over others even though its original density is lower. Given the selector  $S(\mathbf{x})$ , the piece-wise function of the unified field  $F_M : (\mathbf{x}, \mathbf{d}) \rightarrow (\mathbf{c}_S^M, \sigma_S^M)$  can be written as:

$$\sigma_S^M(\mathbf{x}) = \sigma_{S(\mathbf{x})}(\mathbf{M}_{S(\mathbf{x})}\mathbf{x}), \quad (2)$$

$$\mathbf{c}_S^M(\mathbf{x}, \mathbf{d}) = \mathbf{c}_{S(\mathbf{x})}(\mathbf{M}_{S(\mathbf{x})}\mathbf{x}, \mathbf{M}_{S(\mathbf{x})}\mathbf{d}). \quad (3)$$

It is noteworthy to highlight that both  $\mathbf{x}$  and  $\mathbf{d}$  are denoted by homogeneous coordinates. The last element of  $\mathbf{x}$  is 1 while the last element of  $\mathbf{d}$  is 0. With this formulation, the merged radiance field  $F_M(\mathbf{x}, \mathbf{d})$  can be rendered with volumetric rendering [Max 1995]:

$$\hat{\mathbf{C}}(\mathbf{r}(t)) = \sum_{j=1}^K \tau_j \mathbf{c}_S^M(\mathbf{x}_j, \mathbf{d}_j), \quad (4)$$

$$\tau_j = \exp \left( - \sum_{i=1}^{j-1} \sigma_S^M(\mathbf{x}_j) \delta_i \right) \left( 1 - \exp \left( - \sigma_S^M(\mathbf{x}_j) \delta_j \right) \right), \quad (5)$$

where the rendered color  $\hat{\mathbf{C}}(\mathbf{r}(t))$  estimates the image pixel corresponding to the ray  $\mathbf{r}(t) = \mathbf{o} + t\mathbf{d}$ ,  $K$  is the number of samples along  $\mathbf{r}(t)$ ,  $\delta_j$  is the step length of the  $j$ -th sample, and  $\tau_j$  can be seen as the probability that the ray can reach the  $j$ -th sample.

### 3.2 Evaluating Radiance via Closest Ray Sampling

The direct merge of multiple NeRFs is followed by an appearance optimization over the target radiance fields. For each coordinate  $\mathbf{x}$ , rendering its radiance necessitates a view direction  $\mathbf{d}$ . If  $\mathbf{x}$  is sampled from a ray originating from a camera, the process of obtaining the corresponding  $\mathbf{d}$  is straightforward. However, if the goal is to optimize the radiance across the entire 3D space without assuming a specific viewing camera, the view direction  $\mathbf{d}$  is agnostic.

In order to address this challenge, we propose a simple yet effective *Closest Ray Sampling* solution that hinges on sampling the view direction  $\mathbf{d}$  from the entire spectrum of the training dataset. This scheme can match the distribution of view directions with the one seen in the multi-view captures. Specifically, for each point  $\mathbf{x}$ , we determine its view direction as the orientation of the closest training camera ray. Suppose  $\{\mathbf{r}_j(\mathbf{p}_j, \tilde{\mathbf{d}}_j)\}_{j=1}^R$  is the set of all camera rays in the training set. The Euclidean distance  $\|D_{\mathbf{r}_j, \mathbf{x}}\|_2$

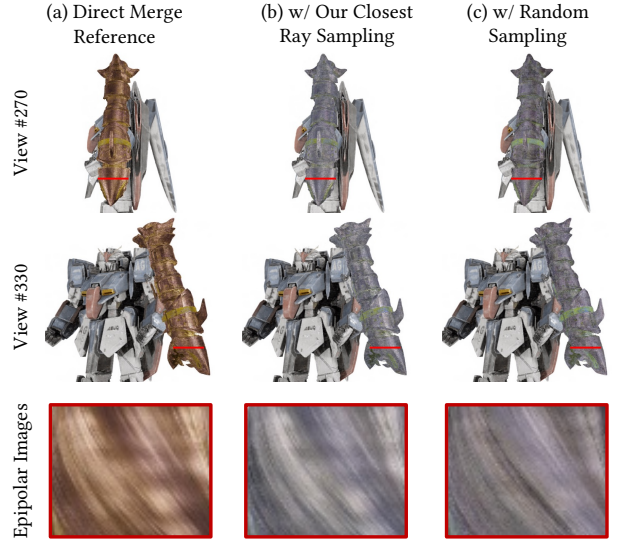


**Figure 3: View-dependent effects on the blended radiance fields via different view-direction sampling schemes.**

between a ray  $\mathbf{r}_j(\mathbf{p}_j, \tilde{\mathbf{d}}_j)$  and a sample point  $\mathbf{x}$  is defined as:

$$p_j^e = \mathbf{p}_j - \left[ (\mathbf{p}_j - \mathbf{x}) \cdot \tilde{\mathbf{d}}_j \right] \tilde{\mathbf{d}}_j, \text{ and } D_{\mathbf{r}_j, \mathbf{x}} = p_j^e - \mathbf{x}, \quad (6)$$

where  $p_j^e$  is the nearest point from the ray  $\mathbf{r}_j$  to the sample point  $\mathbf{x}$ ,  $D_{\mathbf{r}_j, \mathbf{x}} \in \mathbb{R}^3$  is the offset vector from  $\mathbf{x}$  to  $p_j^e$ . The designated view direction for  $\mathbf{x}$  is given as  $\tilde{\mathbf{d}}_j^*$ , where  $j^* = \arg \min_j \|D_{\mathbf{r}_j, \mathbf{x}}\|_2$ .

*Impacts on View-dependent Effects.* View directions are adopted to encode the view-dependent effects, e.g., specular highlights. Therefore, a feasible scheme for sampling view directions is obligated to maintain the view-dependent effects on the original object. Fig. 3 presents a case of shiny object appearance blending. In addition to our proposed scheme, we also provide a straightforward baseline where view directions are randomly sampled. Comparing the reference views (a), our scheme (b) is capable of preserving the original view-dependent specular effects while the baseline scheme (c) smoothens the specular highlights. We also plot (pseudo) epipolar images [Bemana et al. 2022; Verbin et al. 2022] of the red scanline segment. As shown by the last row of Fig. 3, the patterns on the epipolar images obtained through our scheme are more similar to the reference one, in contrast to the baseline scheme.

### 3.3 Boundary Detection and Radiance Pinning

The key to generating seamless NeRFs is to harmonize the color of the target fields with the color of the source field at the boundaries. We draw inspiration from the concept of contact areas to define the boundary regions. Conceptually, these are areas where the density of the radiance field is simultaneously dominated by the source field and the target fields. Formally, we define the boundary regions  $\{\partial B_i\}_{i=2}^N$  as follows:

$$\partial B_i \leftarrow \{\mathbf{x} \mid S(\mathbf{x}) = 1 \text{ and } \sigma_i(\mathbf{M}_i \mathbf{x}) > T_{\text{th}}\}, \quad (7)$$

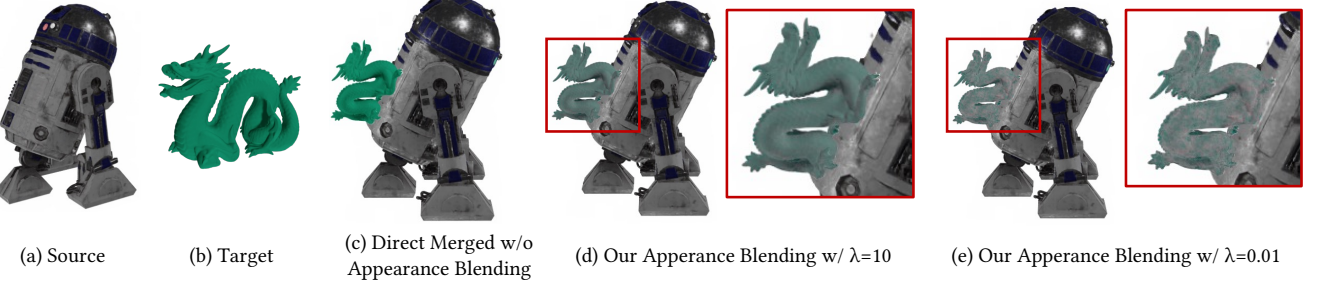


**Figure 4: Ablation study on the weights of gradient loss.** The first two columns (a) and (b) display the source and target objects. The column (c) gives a reference view of direct merge without blending. In (d), we show the blending results under  $\lambda = 10$ . In (e), we show the blending results when decreasing  $\lambda$  to 0.01.



**Figure 5: Ablation study on loss functions.** The column (a) gives two reference views of direct merge. The column (b) shows results when disabling the gradient loss. The column (c) shows results without optimizing the color loss. The column (d) shows results when enabling both the gradient loss and the color loss.

where the threshold  $T_{th}$  signifies the minimal density at which a point in the field is still considered non-empty. This usage is akin to the threshold application in the marching cubes algorithm [Lorensen and Cline 1998], a technique employed for isosurface extraction.

These boundaries  $\partial B_i$  are typically locations where the transition between the source and target radiance fields occurs, and hence, can be potential sites with visual inconsistency when these fields are merged directly. To address this, we introduce a strategy termed *Boundary Radiance Pinning*. The primary objective of this strategy is to minimize the discrepancies between the source field and target fields. Boundary Radiance Pinning functions by enforcing an agreement in radiance color among all target fields and the source field within the boundary region. Specifically, we minimize the loss between the target radiance color and the source radiance color  $c_1(\mathbf{x}, \mathbf{d})$  within the boundary:

$$\mathcal{L}_{color} = \sum_{\mathbf{x} \in \partial B_i} \left\| c_i^M(\mathbf{x}, \mathbf{d}) - c_1(\mathbf{x}, \mathbf{d}) \right\|_2^2. \quad (8)$$

The view direction  $\mathbf{d}$  is obtained by our proposed scheme described in Sec. 3.2. By ensuring alignment in radiance color, appearance continuity on the joined regions is maintained.

### 3.4 Gradient Propagation of Radiance

The boundary radiance pinning will disturb the original details on target fields (see Fig. 5b). In order to preserve the rich textures on the target field, we further add an optimization objective to propagate radiance through the gradient field. The gradients can represent the variation in radiance across different spatial locations. This is particularly critical as many of the patterns and textures are implied in the gradient field of the radiance, as opposed to a single color value. To do this, we first evaluate the gradients of the radiance field within the target regions. This is performed by differentiating the target radiance field w.r.t. the spatial coordinates  $\mathbf{x}$ . After obtaining the gradients of the original target field, we use these gradients as the optimization target for the merged field in the unified global space. The loss function to regularize the gradients of the merged field is formulated as:

$$\mathcal{L}_{grad} = \sum_{\mathbf{x}, S(\mathbf{x}) > 1} \left\| \nabla_{\mathbf{x}} c_S^M(\mathbf{x}, \mathbf{d}) - \nabla_{\mathbf{x}} c_i(M_i \mathbf{x}, M_i \mathbf{d}) \right\|_F^2, \quad (9)$$

where the corresponding view direction  $\mathbf{d}$  can be obtained via the sampling scheme described in Sec. 3.2,  $i = S(\mathbf{x})$  signifies the field index at  $\mathbf{x}$ , and  $\|\cdot\|_F$  is the Frobenius norm. In practice, this involves an iterative optimization procedure, where we aim to fine-tune the target field such that its gradients align with the gradients of the source field at the boundary region and simultaneously maintain the gradient of its original appearance at other regions. However, taking the analytic second-order derivative poses a challenge when using gradient-based optimizers to solve objectives involving gradients. Furthermore, the gradients w.r.t. spatial coordinates  $\mathbf{x}$  are derived from tri-linear interpolation in feature grids, which are not spatially continuous [Li et al. 2023]. In this regard, we opt for a discrete solution. Denote superscript  $k = 1, 2, 3$  as the index of XYZ dimensions. We can calculate the finite difference in radiance color at the position  $\mathbf{x}$  by:

$$\mathcal{V}_{\mathbf{x}^k} = c_i(M_i \mathbf{x}, M_i \mathbf{d}) - c_i(M_i(\mathbf{x} + \Delta_k), M_i \mathbf{d}). \quad (10)$$

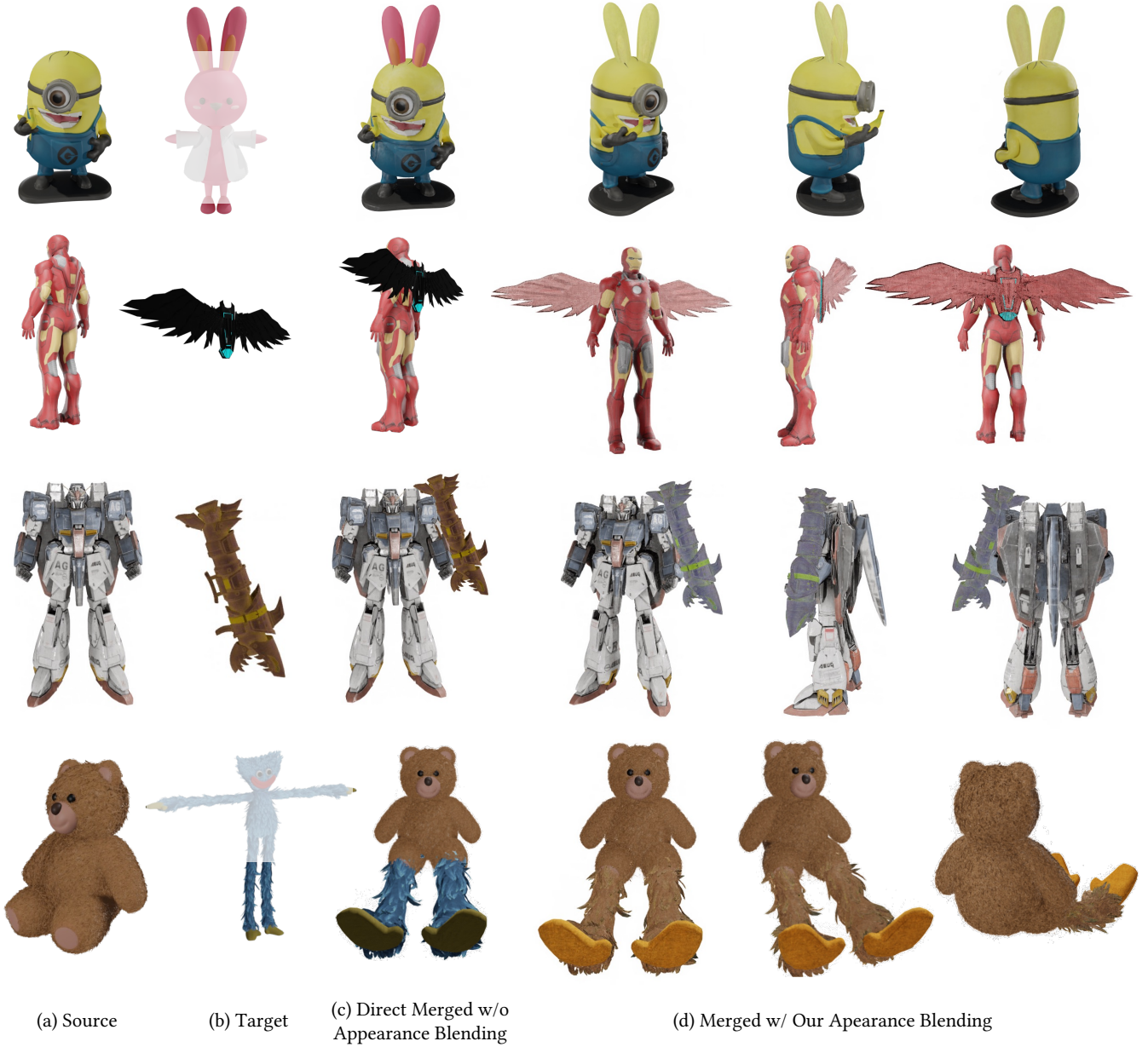


**Figure 6: Showcase of our apperance blending results.** In (a) and (b), we present reference images of source and target radiance fields, respectively. The column (c) shows results of direct merge of the source and target. The last three columns in (d) exhibit three views of the merged and appearance blended radiance fields.

Here,  $\mathbf{x} + \Delta_k$  is a neighborhood point of  $\mathbf{x}$  along the  $k$ -th dimension. Then we obtain the discrete version of gradient loss:

$$\mathcal{L}_{grad} = \sum_{\mathbf{x}, S(\mathbf{x}) > 1} \sum_{k=1}^3 \left\| \mathbf{c}_S^M(\mathbf{x}, \mathbf{d}) - \mathbf{c}_S^M(\mathbf{x} + \Delta_k, \mathbf{d}) - \nabla_{\mathbf{x}^k} \right\|_2^2. \quad (11)$$

In the above equation, the difference between  $\mathbf{c}_S^M(\mathbf{x}, \mathbf{d})$  and  $\mathbf{c}_S^M(\mathbf{x} + \Delta_k, \mathbf{d})$  approximates the radiance gradient of the merged field at

the position  $\mathbf{x}$  along the  $k$ -th dimension. The sum is taken over all sample points in the merged field and XYZ dimensions.

By minimizing this gradient loss, the textures and patterns implied in the gradient field can be preserved. Meanwhile, the color scheme from the source field can be propagated to the target fields, resulting in a seamless transition of radiance across the boundary.



**Figure 7: Comparisons between our approach and baseline methods.** For the first case, the baseline StyleRF [Liu et al. 2023] stylizes the target radiance fields with the source one. For the second case, we adopt SDEdit [Meng et al. 2021] to perform text-guided image-to-image generation of target radiance field renderings.

### 3.5 Optimization and Network Architecture

To establish the final objective function, we combine the gradient loss with the color loss. The overall loss of our optimization process is formulated as a weighted sum, defined as follows:

$$\mathcal{L} = \mathcal{L}_{color} + \lambda \mathcal{L}_{grad}. \quad (12)$$

In this equation, the parameter  $\lambda$  is utilized to balance the relative contribution of color loss and gradient loss to the overall objective. In our experiments, we set the value of  $\lambda$  as 0.1.

To conduct the appearance optimization of the target fields, we introduce a ControlNet-style [Zhang and Agrawala 2023] architecture to facilitate the fine-tuning process. This involves adopting the original network parameters as the initialization of a trainable copy and appending a “zero convolution” to connect the trainable copy to the original networks as a render branch. During the appearance blending process, the parameters of the original networks will be frozen, serving as an initial model and evaluator of the original gradient field. The ControlNet-style network branch is introduced to learn the incremental modifications, which are added to the original appearance via the “zero convolution”. The choice of “zero convolution” stems from its ability to retain the original output and progressively fuse modifications to the appearance at the beginning of fine-tuning. Fig. 2 presents the entire pipeline of our method.

## 4 EXPERIMENTS

To evaluate the performance of our proposed approach, our experiments are conducted on multiple 3D models from the Objaverse [Deitke et al. 2023] dataset. Our implementation is built on the backbone of TensoRF. Nevertheless, since our approach operates directly on the output of radiance fields, it does not depend on specific radiance field modeling. Results of our approach with Naïve NeRF [Mildenhall et al. 2021], Instant-NGP [Müller et al. 2022], and DirectVoxGO [Sun et al. 2022b] backbones are present in Fig. 10.



**Figure 8: Color scheme cloning results via our appearance blending approach.**



**Figure 9: Ablation study on different configurations of the trainable copy.**

### 4.1 Qualitative Comparison

Since there is no existing method of seamless appearance blending in the context of radiance fields, we build two baselines with recent emerging techniques to validate the effectiveness of our approach. The first baseline attempts to perform 3D style transfer from the source to target. We train StyleRF [Liu et al. 2023] for zero-shot NeRF stylization. For the second baseline, we utilize the diffusion model to conduct image-to-image generation [Meng et al. 2021] guided by an editing text prompt and rendered images. Fig. 7 shows two comparison cases. In the first case, StyleRF fails to seamlessly transfer the color scheme from the “Minion” to the “rabbit ear” since it is not capable of extracting style information from an ordinary image. In the second case, we use a text prompt to generate a view based on the original rendering in order to match our editing goal. We can see the generated “wing” contains elements of “Ironman” but still fails to yield a seamless merge.

### 4.2 Ablation Study

*Gradient Loss for Radiance Propagation.* As demonstrated in Fig. 5b, upon removing the gradient loss function, we observed a remarkable deterioration in the quality of radiance propagation, resulting in artifacts on the texture. After adding the gradient loss, the small details on the texture implied in the gradient field are well preserved. Moreover, Fig. 4 shows the impacts of the gradient loss weight. When imposing a strong constraint ( $\lambda = 10$ ), the radiance gradients are maintained while the impacts from the source object are weakened. When decreasing the weight to 0.01, the appearance from the source object dominates the appearance blending and violates the original radiance gradients.

*Boundary Radiance Pinning.* In this study, we opted to omit the color loss component in our objective to analyze the impacts of boundary radiance pinning. Fig. 5c displays the result without the color loss. Since boundary pinning is disabled, the target radiance field will be optimized through mixed gradients from the source field, which harms the rich lighting and textual details in the original target field. Thus, combining color loss and gradient loss can achieve the best blending performance.

*Configurations of Trainable Copies.* We also ablate different trainable copy configurations. Our TensoRF-VM [Chen et al. 2022a] backbone consists of VM (vector-matrices) factors and shading MLPs, where VM factors compute the feature of each query point and shading MLPs render the feature into RGB color. Fig. 9 shows that the blending performance will compromise when freezing the VM factors and only optimizing the shading module. Thus, trainable VM copy is essential for high-quality blending.

### 4.3 Visual Results and Applications

We showcase the results of our SeamlessNeRF on multiple cases, as exhibited in Fig. 6. We can see that the our approach can generate seamless part NeRF stitching on various challenging cases. We also include the visualizations of the optimization process in Fig. 11.

*Applications.* Our proposed approach demonstrates the potential for expansion into 3D creation and editing workflows, offering advantages in the productivity of 3D modeling. For instance, consider the scenario where artists intend to restore the arms of the “Venus de Milo” sculpture, as shown in Fig. 1. In such a case, our approach enables the seamless blending of pre-existing arm assets onto the sculpture, expediting the modeling process compared to starting from scratch. As a more practical case, the “Toad Temple” in Fig. 5d exhibits a building model stitched from two existing 3D assets, which can be employed as a game element. Users can also customize cartoon characters (the first case in Fig. 6) without time-consuming modeling and re-texturing. In addition, Fig. 8 illustrates a color scheme transferring application of our approach, where the target objects clone the appearance of the source objects.

## 5 CONCLUSION

This paper presents SeamlessNeRF, a novel approach to seamless stitching of multiple NeRFs into a unified 3D scene. By extending the principles of gradient-domain blending to NeRFs, our method can propagate appearance from the source field to the target field. Our experiments validate the effectiveness of our approach in achieving seamless merges across diverse objects. The successful application of Poisson Editing to NeRFs represents a significant advancement in the realm of 3D scene composition and editing.

*Limitations and Future Work.* Since our current work doesn’t explicitly factor in lighting, it may struggle to handle the cases when the lighting and material properties of the source and target fields are inconsistently matched. To disentangle the impacts of lighting, we can apply our propagation to the albedo component with a NeRF backbone supporting decomposed lighting and materials, which is a promising topic for future work.

## ACKNOWLEDGMENTS

This work was supported in part by Science, Technology and Innovation Commission of Shenzhen Municipality Project No. SGDX20220530111201008, in part by Hong Kong Research Grants Council Project No. T45-401/22-N, in part by NSFC-62172348, in part by Outstanding Young Fund of Guangdong Province with No. 2023B1515020055, in part by Shenzhen General Project with No. JCYJ20220530143604010, and in part by CCF-Tencent Open Research Fund. This work used and adapted 3D models created and shared by Coen.Fransen (CC BY), Nikolai Jónasson (CC BY), hanjum (CC BY), mwilson1 (CC BY), fongoose (CC BY-NC), jesuskrisis (CC BY), Edward Johnson 3 (CC BY), cosmos28 (CC BY), firmasyahh (CC BY), SamkyClance (CC BY), Hristo (CC BY), Maurice Svay (CC BY), racush (CC BY), and David Wigforss (CC BY).

## REFERENCES

- Aseem Agarwala, Mira Dontcheva, Maneesh Agrawala, Steven Drucker, Alex Colburn, Brian Curless, David Salesin, and Michael Cohen. 2004. Interactive Digital Photomontage. In *ACM SIGGRAPH 2004 Papers* (Los Angeles, California) (*SIGGRAPH '04*). Association for Computing Machinery, New York, NY, USA, 294–302. <https://doi.org/10.1145/1186562.1015718>
- Connelly Barnes, Eli Shechtman, Adam Finkelstein, and Dan B Goldman. 2009. Patch-Match: A Randomized Correspondence Algorithm for Structural Image Editing. *ACM Trans. Graph.* 28, 3, Article 24 (jul 2009), 11 pages. <https://doi.org/10.1145/1531326.1531330>
- Mojtaba Bemana, Karol Myszkowski, Jeppe Revall Frisvad, Hans-Peter Seidel, and Tobias Ritschel. 2022. Eikonal fields for refractive novel-view synthesis. In *ACM SIGGRAPH 2022 Conference Proceedings*, 1–9.
- Pravin Bhat, C. Lawrence Zitnick, Michael F. Cohen, and Brian Curless. 2010. GradientShop: A gradient-domain optimization framework for image and video filtering. *ACM Trans. Graph.* 29 (2010), 10:1–10:14.
- Mark Boss, Andreas Engelhardt, Abhishek Kar, Yuanzhen Li, Deqing Sun, Jonathan Barron, Hendrik Lensch, and Varun Jampani. 2022. Samurai: Shape and material from unconstrained real-world arbitrary image collections. *Advances in Neural Information Processing Systems* 35 (2022), 26389–26403.
- Tim Brooks, Aleksander Holynski, and Alexei A Efros. 2023. Instructpix2pix: Learning to follow image editing instructions. In *Proceedings of the IEEE/CVF Conference on Computer Vision and Pattern Recognition*, 18392–18402.
- Anpei Chen, Zexiang Xu, Andreas Geiger, Jingyi Yu, and Hao Su. 2022a. TensoRF: Tensorial Radiance Fields. In *Computer Vision – ECCV 2022*. Shai Avidan, Gabriel Brostow, Moustapha Cissé, Giovanni Maria Farinella, and Tal Hassner (Eds.). Springer Nature Switzerland, Cham, 333–350.
- Yaosen Chen, Qi Yuan, Zhiqiang Li, Yuegen Liu, Wei Wang, Chaoping Xie, Xuming Wen, and Qien Yu. 2022b. UPST-NeRF: Universal Photorealistic Style Transfer of Neural Radiance Fields for 3D Scene. *arXiv preprint arXiv:2208.07059* (2022).
- Soheil Darabi, Eli Shechtman, Connelly Barnes, Dan B. Goldman, and Pradeep Sen. 2012. Image melding. *ACM Transactions on Graphics (TOG)* 31 (2012), 1 – 10.
- Matt Deitke, Dustin Schwenk, Jordi Salvador, Luca Weihs, Oscar Michel, Eli VanderBilt, Ludwig Schmidt, Kiana Ehsani, Aniruddha Kembhavi, and Ali Farhadi. 2023. Objaverse: A universe of annotated 3d objects. In *Proceedings of the IEEE/CVF Conference on Computer Vision and Pattern Recognition*, 13142–13153.
- Arnaud Dessein, William AP Smith, Richard C Wilson, and Edwin R Hancock. 2014. Seamless texture stitching on a 3D mesh by poisson blending in patches. In *2014 IEEE International Conference on Image Processing (ICIP)*. IEEE, 2031–2035.
- Zhiwen Fan, Yifan Jiang, Peihao Wang, Xinyu Gong, Dejia Xu, and Zhangyang Wang. 2022. Unified Implicit Neural Styling. In *Computer Vision – ECCV 2022*, Shai Avidan, Gabriel Brostow, Moustapha Cissé, Giovanni Maria Farinella, and Tal Hassner (Eds.). Springer Nature Switzerland, Cham, 636–654.
- Bingchen Gong, Yuehao Wang, Xiaoguang Han, and Qi Dou. 2023. RecolorNeRF: Layer Decomposed Radiance Field for Efficient Color Editing of 3D Scenes. *arXiv preprint arXiv:2301.07958* (2023).
- Ayaan Haque, Matthew Tancik, Alexei A Efros, Aleksander Holynski, and Angjoo Kanazawa. 2023. Instruct-NeRF2NeRF: Editing 3D Scenes with Instructions. *arXiv preprint arXiv:2303.12789* (2023).
- Clément Jambon, Bernhard Kerbl, Georgios Kopanas, Stavros Diolatzis, Thomas Leimkühler, and George Drettakis. 2023. NeRFshop: Interactive Editing of Neural Radiance Fields”. *Proceedings of the ACM on Computer Graphics and Interactive Techniques* 6, 1 (May 2023). <https://repo-sam.inria.fr/fungraph/nerfshop/>
- Biliana Kaneva, Josef Sivic, Antonio Torralba, Shai Avidan, and William T. Freeman. 2010. Infinite Images: Creating and Exploring a Large Photorealistic Virtual Space. *Proc. IEEE* 98, 8 (2010), 1391–1407. <https://doi.org/10.1109/JPROC.2009.2031133>

- Sosuke Kobayashi, Eiichi Matsumoto, and Vincent Sitzmann. 2022. Decomposing NeRF for Editing via Feature Field Distillation. In *Advances in Neural Information Processing Systems*, S. Koyejo, S. Mohamed, A. Agarwal, D. Belgrave, K. Cho, and A. Oh (Eds.), Vol. 35. Curran Associates, Inc., 23311–23330. <https://proceedings.neurips.cc/paper/2022/file/93f250215e4889119807bfefac3a57aec-Paper-Conference.pdf>
- Zhengfei Kuang, Fujun Luan, Sai Bi, Zhixin Shu, Gordon Wetzstein, and Kalyan Sunkavalli. 2023. Palettenerf: Palette-based appearance editing of neural radiance fields. In *Proceedings of the IEEE/CVF Conference on Computer Vision and Pattern Recognition*. 20691–20700.
- Vivek Kwatra, Irfan Essa, Aaron Bobick, and Nipun Kwatra. 2005. Texture Optimization for Example-Based Synthesis. *ACM Trans. Graph.* 24, 3 (jul 2005), 795–802. <https://doi.org/10.1145/1073204.1073263>
- Zhaoshuo Li, Thomas Müller, Alex Evans, Russell H Taylor, Mathias Unberath, Ming-Yu Liu, and Chen-Hsuan Lin. 2023. Neuralangelo: High-Fidelity Neural Surface Reconstruction. In *Proceedings of the IEEE/CVF Conference on Computer Vision and Pattern Recognition*. 8456–8465.
- Jing Liao, Yuan Yao, Lu Yuan, Gang Hua, and Sing Bing Kang. 2017. Visual Attribute Transfer through Deep Image Analogy. *ACM Trans. Graph.* 36, 4, Article 120 (jul 2017), 15 pages. <https://doi.org/10.1145/3072959.3073683>
- Kunhao Liu, Fangneng Zhan, Yiwen Chen, Jiahui Zhang, Yingchen Yu, Abdulkotaleb El Saddik, Shijian Lu, and Eric P Xing. 2023. StyleRF: Zero-shot 3D Style Transfer of Neural Radiance Fields. In *Proceedings of the IEEE/CVF Conference on Computer Vision and Pattern Recognition*. 8338–8348.
- Steven Liu, Xiuming Zhang, Zhoutong Zhang, Richard Zhang, Jun-Yan Zhu, and Bryan Russell. 2021. Editing Conditional Radiance Fields. In *Proceedings of the IEEE/CVF International Conference on Computer Vision (ICCV)*. 5773–5783.
- William E Lorensen and Harvey E Cline. 1998. Marching cubes: A high resolution 3D surface construction algorithm. In *Seminal graphics: pioneering efforts that shaped the field*. 347–353.
- Nelson Max. 1995. Optical models for direct volume rendering. *IEEE Transactions on Visualization and Computer Graphics* 1, 2 (1995), 99–108.
- Chenlin Meng, Yang Song, Jiaming Song, Jiajun Wu, Jun-Yan Zhu, and Stefano Ermon. 2021. Sdedit: Image synthesis and editing with stochastic differential equations. *arXiv preprint arXiv:2108.01073* (2021).
- Ben Mildenhall, Pratul P. Srinivasan, Matthew Tancik, Jonathan T. Barron, Ravi Ramamoorthi, and Ren Ng. 2021. NeRF: Representing Scenes as Neural Radiance Fields for View Synthesis. *Commun. ACM* 65, 1 (dec 2021), 99–106. <https://doi.org/10.1145/3503250>
- Thomas Müller, Alex Evans, Christoph Schied, and Alexander Keller. 2022. Instant Neural Graphics Primitives with a Multiresolution Hash Encoding. *ACM Trans. Graph.* 41, 4, Article 102 (jul 2022), 15 pages. <https://doi.org/10.1145/3528223.3530127>
- Jacob Munkberg, Jon Hasselgren, Tianchang Shen, Jun Gao, Wenzheng Chen, Alex Evans, Thomas Müller, and Sanja Fidler. 2022. Extracting Triangular 3D Models, Materials, and Lighting From Images. In *Proceedings of the IEEE/CVF Conference on Computer Vision and Pattern Recognition (CVPR)*. 8280–8290.
- Patrick Pérez, Michel Gangnet, and Andrew Blake. 2003. Poisson image editing. *ACM SIGGRAPH 2003 Papers* (2003).
- Alec Radford, Jong Wook Kim, Chris Hallacy, Aditya Ramesh, Gabriel Goh, Sandhini Agarwal, Girish Sastry, Amanda Askell, Pamela Mishkin, Jack Clark, Gretchen Krueger, and Ilya Sutskever. 2021. Learning Transferable Visual Models From Natural Language Supervision. In *Proceedings of the 38th International Conference on Machine Learning (Proceedings of Machine Learning Research, Vol. 139)*, Marina Meila and Tong Zhang (Eds.). PMLR, 8748–8763. <https://proceedings.mlr.press/v139/radford21a.html>
- Claudio Rocchini, Paolo Cignoni, Claudio Montani, and Roberto Scopigno. 1999. Multiple textures stitching and blending on 3D objects. In *Rendering Techniques' 99: Proceedings of the Eurographics Workshop in Granada, Spain, June 21–23, 1999*. Springer, 119–130.
- Pratul P Srinivasan, Boyang Deng, Xiuming Zhang, Matthew Tancik, Ben Mildenhall, and Jonathan T Barron. 2021. Nerv: Neural reflectance and visibility fields for re-lighting and view synthesis. In *Proceedings of the IEEE/CVF Conference on Computer Vision and Pattern Recognition*. 7495–7504.
- Chunyi Sun, Yanbing Liu, Junlin Han, and Stephen Gould. 2022a. NeRFEditor: Differentiable Style Decomposition for Full 3D Scene Editing. *arXiv preprint arXiv:2212.03848* (2022).
- Cheng Sun, Min Sun, and Hwann-Tzong Chen. 2022b. Direct Voxel Grid Optimization: Super-Fast Convergence for Radiance Fields Reconstruction. In *Proceedings of the IEEE/CVF Conference on Computer Vision and Pattern Recognition (CVPR)*. 5459–5469.
- Matthew Tancik, Vincent Casser, Xinchen Yan, Sabeek Pradhan, Ben Mildenhall, Pratul P Srinivasan, Jonathan T Barron, and Henrik Kretzschmar. 2022. Blocknerf: Scalable large scene neural view synthesis. In *Proceedings of the IEEE/CVF Conference on Computer Vision and Pattern Recognition*. 8248–8258.
- Jiaxiang Tang, Xiaokang Chen, Jingbo Wang, and Gang Zeng. 2022. Compressible-composable NeRF via Rank-residual Decomposition. In *Advances in Neural Information Processing Systems*, S. Koyejo, S. Mohamed, A. Agarwal, D. Belgrave, K. Cho, and A. Oh (Eds.), Vol. 35. Curran Associates, Inc., 14798–14809. <https://proceedings.neurips.cc/paper/2022/file/5ed5c3c846f684a54975ad7a2525199f-Paper-Conference.pdf>
- Dor Verbin, Peter Hedman, Ben Mildenhall, Todd Zickler, Jonathan T. Barron, and Pratul P. Srinivasan. 2022. Ref-NeRF: Structured View-Dependent Appearance for Neural Radiance Fields. In *Proceedings of the IEEE/CVF Conference on Computer Vision and Pattern Recognition (CVPR)*. 5491–5500.
- Can Wang, Menglei Chai, Mingming He, Dongdong Chen, and Jing Liao. 2022. CLIP-NeRF: Text-and-Image Driven Manipulation of Neural Radiance Fields. In *Proceedings of the IEEE/CVF Conference on Computer Vision and Pattern Recognition (CVPR)*. 3835–3844.
- Hongcheng Wang, Ning Xu, Ramesh Raskar, and Narendra Ahuja. 2007. Videoshop: A new framework for spatio-temporal video editing in gradient domain. *Graphical Models* 69, 1 (2007), 57–70. <https://doi.org/10.1016/j.gmod.2006.06.002>
- Dejia Xu, Peihai Wang, Yifan Jiang, Zhiwen Fan, and Zhangyang Wang. 2022. Signal Processing for Implicit Neural Representations. In *Advances in Neural Information Processing Systems*, S. Koyejo, S. Mohamed, A. Agarwal, D. Belgrave, K. Cho, and A. Oh (Eds.), Vol. 35. Curran Associates, Inc., 13404–13418. <https://proceedings.neurips.cc/paper/2022/file/575c450013d0e99e4b0ecf82bd1faa4-Paper-Conference.pdf>
- Bangbang Yang, Yinda Zhang, Yinghao Xu, Yijin Li, Han Zhou, Hujun Bao, Guofeng Zhang, and Zhaopeng Cui. 2021. Learning Object-Compositional Neural Radiance Field for Editable Scene Rendering. In *Proceedings of the IEEE/CVF International Conference on Computer Vision (ICCV)*. 13779–13788.
- Yizhou Yu, Kun Zhou, Dong Xu, Xiaohan Shi, Hujun Bao, Baining Guo, and Heung-Yeung Shum. 2004. Mesh Editing with Poisson-Based Gradient Field Manipulation. In *ACM SIGGRAPH 2004 Papers* (Los Angeles, California) (*SIGGRAPH '04*). Association for Computing Machinery, New York, NY, USA, 644–651. <https://doi.org/10.1145/1186562.1015774>
- Yu-Jie Yuan, Yang-Tian Sun, Yu-Kun Lai, Yuewen Ma, Rongfei Jia, and Lin Gao. 2022. NeRF-Edition: Geometry Editing of Neural Radiance Fields. In *Proceedings of the IEEE/CVF Conference on Computer Vision and Pattern Recognition (CVPR)*. 18353–18364.
- Jiakai Zhang, Xinhang Liu, Xinyi Ye, Fuqiang Zhao, Yanshun Zhang, Minye Wu, Yingliang Zhang, Lan Xu, and Jingyi Yu. 2021a. Editable Free-Viewpoint Video Using a Layered Neural Representation. *ACM Trans. Graph.* 40, 4, Article 149 (jul 2021), 18 pages. <https://doi.org/10.1145/3450626.3459756>
- Kai Zhang, Nick Kolkin, Sai Bi, Fujun Luan, Zexiang Xu, Eli Shechtman, and Noah Snavely. 2022. ARF: Artistic Radiance Fields. In *Computer Vision – ECCV 2022*, Shai Avidan, Gabriel Brostow, Moustapha Cissé, Giovanni Maria Farinella, and Tal Hassner (Eds.). Springer Nature Switzerland, Cham, 717–733.
- Lvmin Zhang and Maneesh Agrawala. 2023. Adding Conditional Control to Text-to-Image Diffusion Models. *arXiv:2302.05543 [cs.CV]*
- Xiuming Zhang, Pratul P Srinivasan, Boyang Deng, Paul Debevec, William T Freeman, and Jonathan T Barron. 2021b. Nerfactor: Neural factorization of shape and reflectance under an unknown illumination. *ACM Transactions on Graphics (ToG)* 40, 6 (2021), 1–18.
- Chengwei Zheng, Wenbin Lin, and Feng Xu. 2022. EditableNeRF: Editing Topologically Varying Neural Radiance Fields by Key Points. *arXiv preprint arXiv:2212.04247* (2022).
- Yiyu Zhuang, Hao Zhu, Xusen Sun, and Xun Cao. 2022. MoFaNeRF: Morphable Facial Neural Radiance Field. In *Computer Vision – ECCV 2022*, Shai Avidan, Gabriel Brostow, Moustapha Cissé, Giovanni Maria Farinella, and Tal Hassner (Eds.). Springer Nature Switzerland, Cham, 268–285.



**Figure 10: Appearance blending results with the three backbones.** Our method can be implemented across various radiance field backbone. Although NeRF variants differ in radiance field parameterization, they all encode scenes as a mapping from coordinates to densities and RGB values via differentiable neural encodings. As our approach operates directly on the output, specific parameterizations do not impact our gradient-based blending framework. In addition to TensoRF which has been already used in our main experiments, we test our approach on Naive NeRF [Mildenhall et al. 2021], Instant-NGP [Müller et al. 2022], and DirectVoxGO [Sun et al. 2022b].

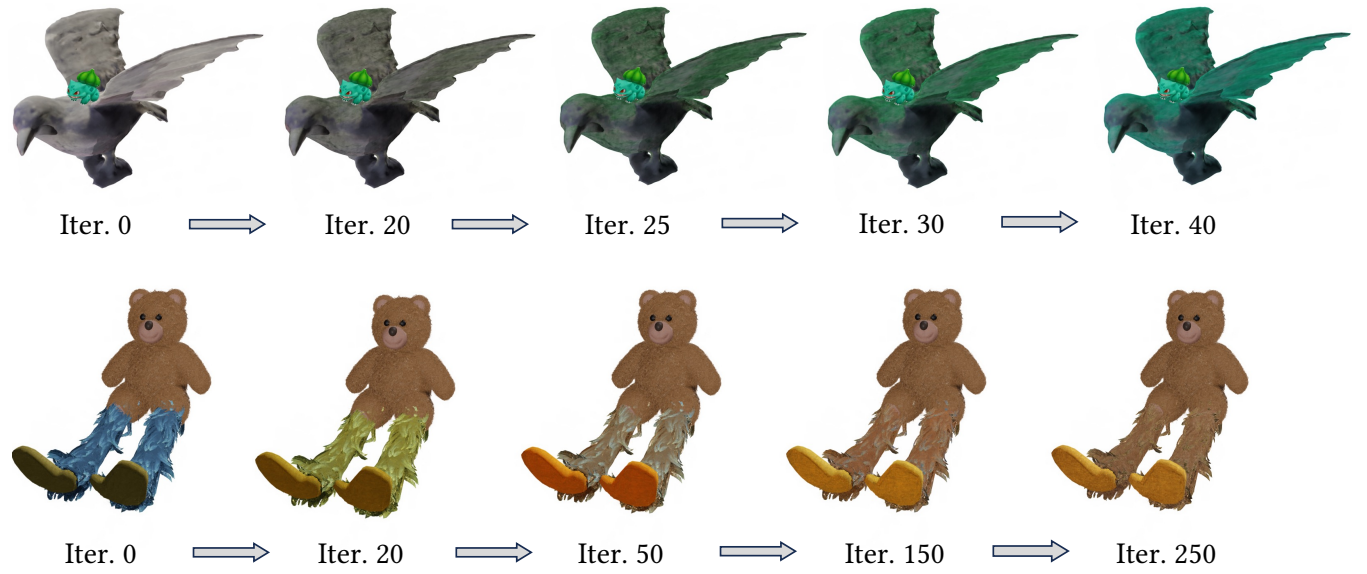


**Figure 11: Visualizes the fine-tuning processes of two representative cases.** The fine-tuning of the simpler case (the first row) will converge within 50 iterations. While the case with more complex textures (the second row) consumes more fine-tuning time to simultaneously optimize the gradient loss and color loss.